5

A Robust Traction Control for Electric Vehicles Without Chassis Velocity

Jia-Sheng Hu[1], Dejun Yin[2] and Feng-Rung Hu[3]
[1]*National University of Tainan,*
[2]*Keio University,*
[3]*National Taichung University,*
[1,3]*Taiwan*
[2]*Japan*

1. Introduction

As the rapid development of technology, the control technology and daily livings are interrelated. However, unanticipated breakdowns can happen in any control system due to the internal malfunctions or external distractions. Since the prices in most of the home electronic appliances are reasonable and affordable, malfunctions can simply be solved by purchasing new ones, however, for complex control systems with high social costs, the consequences of these passive solutions result in paying more prices. For example, systems such as aircrafts, ships, satellites, nuclear power plants, space shuttles, high speed rails are all extremely high in manufacturing costs, and if malfunction happens and is not able to eliminate or repair, the price paying afterward is tremendous.

Traction control is an example. For passenger involved in electric automobile systems, traction control is a core for stabilizing the movements of automobiles. In addition to guarantee the safety of automobile system in any driving conditions, one must also has adequate ability of fault-tolerant. Under a slippery, a muddy, and a flat tire conditions, wheel inertia changes, and results in deteriorating of controllability in traction control. Hence, researches have been focusing on adopting robust control theory, which can endow electric vehicles with fault-tolerant performance. Fully electric vehicles powered by batteries can achieve quieter and pollution-free operation, which has offered a solution to next generation vehicles. Unlike internal combustion engine vehicles, electric vehicles use independently equipped motors to drive each wheel. The independently equipped motors provide higher power/weight density, higher reliability for safety and better dynamic performance. These aspects make it easy to estimate the driving or braking forces between tires and road surfaces in real time, which contributes a great deal to the application of new traction control strategies based on road condition estimation (Hori, 2004; He & Hori, 2006; Yang & Lo, 2008).

For advanced vehicles today, many technologies embedded in the micro controller unit (MCU) that enhance the vehicle stability and handling performance in critically dynamic situations. For example, the antilock braking system (ABS) (Schinkel & Hunt, 2002; Patil et al., 2003), electronic differential (ED) (Urakubo et al., 2001; Tsai & Hu, 2007), direct yaw-

posture control (DYC) (Tahami et al., 2004; Mizushima et al., 2006), traction control (Bennett et al., 1999; Poursamad & Montazeri, 2008), and so on, are all solutions implemented to improve both vehicle stability and handling. Traction control is often interested in the performance of anti-slip mechanisms. When a vehicle is driven or brakes on a slippery road, traction control must not only guarantee the effectiveness of the torque output to maintain vehicle stability, but also provide some information about tire-road conditions to other vehicle control systems. Moreover, a well-managed traction control system can cover the functions of ABS, because motors can generate deceleration torque as easily as acceleration one (Mutoh et al., 2007). However, in practice, vehicle systems actually face challenges on restricting the development of traction control. For example, when the real chassis velocity is not available, the friction force which drives the vehicle is immeasurable (Baffet et al., 2009). In general traction control systems that need chassis velocity, the non-driven wheels are utilized to provide an approximate vehicle velocity due to physical and economic reasons. However, this method is not applicable when the vehicle is accelerated by 4WD systems or decelerated by brakes equipped in these wheels. For this reason, the accelerometer measurement is also used to calculate the velocity value, but it cannot avoid offset and error problems. Other sensors, e.g., optical sensors (Saito et al., 2002), sensors of magnetic markers (Fujimoto et al., 2004), etc., can also obtain chassis velocity. However, they are too sensitive and reliant on the driving environment or too expensive to be applied in actual vehicles. Some anti-slip control systems (Schinkel & Hunt, 2002; Patil et al., 2003; Fujii & Fujimoto, 2007) try to realize optimal slip-ratio controls according to the Magic Formula (Pacejka & Bakker, 1992). These systems not only need extra sensors for the acquisition of chassis velocity or acceleration, but are also more difficult to realize than expected. This is because the tuned algorithms and parameters for specific tire-road conditions cannot be adapted quickly enough to compensate the significant variation found in the instantaneous, immeasurable relationship between the slip ratio and the friction coefficient. In order to overcome these problems, the Model Following Control (MFC) approaches (Sakai & Hori, 2001; Saito et al., 2002; Fujimoto et al., 2004), do not need information on chassis velocity or even acceleration sensors are proposed. In these systems, the controllers only make use of torque and wheel rotation as input variables for calculation. Fewer sensors contribute not only to lower costs, but also to increase reliability and independence from driving conditions, which are the most outstanding features of this class of control systems. Nevertheless, these control designs based on compensation have to consider the worst stability case to decide the compensation gain, which impairs the performance of anti-slip control. Furthermore, gain tuning for some specific tire-road conditions also limits the practicability of this method. Recently, the MTTE approach (Yin et al., 2009) that requires neither chassis velocity nor information about tire-road conditions further upgrades the anti-slip performance of electric vehicles. In this system, use is only made of the torque reference and the wheel rotation speed to estimate the maximum transmissible torque to the road surface, then the estimated torque is applied for anti-slip control implementation. This approach also shows its benefits for vehicle mass-perturbed operation. Since a human being is involved in the operation of a vehicle, the total mass potentially varies with different drivers and passengers.

Model uncertainties are considered as systematic faults (Patton et al., 2000; Campos-Delgado et al., 2005), and these faults are unpreventable and non-measurable in automobile control systems. Normally, due to the existence of different levels of faults in general automobile

control system, the anti-slip function of traction control will deteriorate and even malfunction occur (Ikeda et al., 1992). For example, different passengers are with different weights, and this causes the vehicle mass to be unpredictable. In addition, the wheel inertia changes because of abrasion, repairs, tire flattening, and practical adhesion of mud and stones. For traction control, these two factors have significant impacts on anti-slip function in traction control. Additionally, feedback control is established upon the output measurement. Sensor faults deteriorate the measurement signals and decline the stability. Therefore, a fine traction control of electric vehicle should equip the ability of fault-tolerant against these faults. Truly, to develop traction control with fault-tolerant technique is practically competitive. This paper aims to make use of the advantages of electric vehicles to discuss the robustness of MTTE-based traction control systems and is structured as follows. Section 2 describes the MTTE approach for anti-slip control. Section 3 discusses the concepts of disturbance estimation. Details of the robustness analysis to the discussed systems are presented in Section 4. The specifications of the experiments and practical examples for evaluating the presented anti-slip strategy are given in Section 5. Finally, Section 6 offers some concluding remarks.

2. Traction control without chassis velocity

Consider a longitudinal motion of a four-wheeled vehicle, as depicted in Fig. 1, the dynamic differential equations for the longitudinal motion of the vehicle can be described as

$$J_w\dot{\omega} = T - rF_d \tag{1}$$

$$M\dot{V} = F_d - F_{dr} \tag{2}$$

$$V_w = r\omega \tag{3}$$

$$F_d(\lambda) = \mu N \tag{4}$$

Generally, the nonlinear interrelationships between the slip ratio λ and friction coefficient μ formed by tire's dynamics can be modeled by the widely adopted Magic Formula (Pacejka & Bakker, 1992) as shown in Fig. 2.

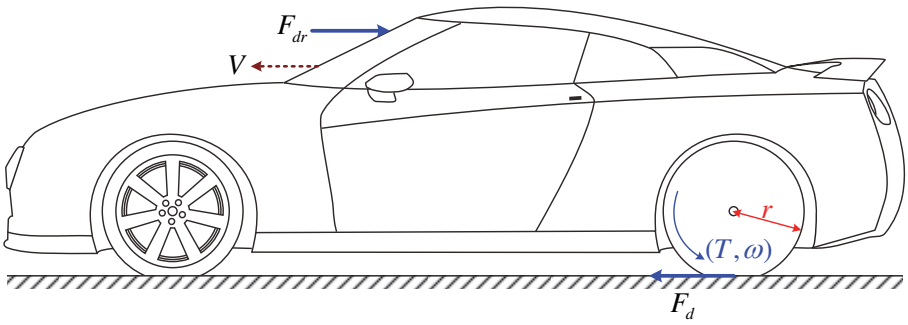

Fig. 1. Dynamic longitudinal model of vehicle.

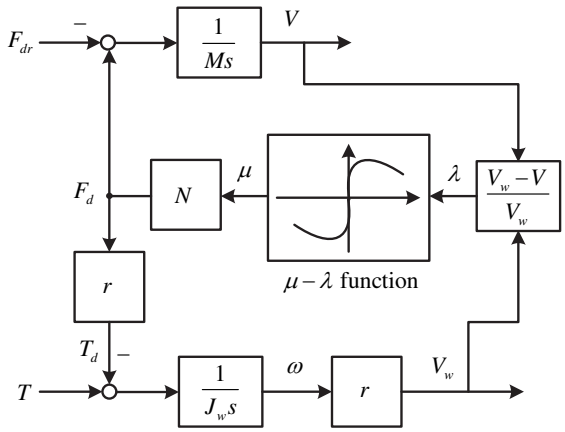

Fig. 2. One wheel of vehicle model with magic formula.

The concept of MTTE approach for vehicle anti-slip control is firstly proposed in (Yin et al., 2009). The MTTE approach can achieve an acceptable anti-slip control performance under common operation requirements. However, the MTTE approach is sensitive to the varying of the wheel inertia. If the wheel inertia varies, the anti-slip performance of the MTTE will deteriorate gradually. This paper is devoted to improve the anti-slip performance of the MTTE approach under such concerned abnormal operations. An advanced MTTE approach with fault-tolerant performance is then proposed. Based on the MTTE approaches, the following considerations are concerned.

1. No matter what kind of tire-road condition the vehicle is driven on, the kinematic relationship between the wheel and the chassis is always fixed and known.
2. During the acceleration phase, considering stability and tire abrasion, well-managed control of the velocity difference between wheel and chassis is more important than the mere pursuit of absolute maximum acceleration.
3. If the wheel and the chassis accelerations are well controlled, the difference between the wheel and the chassis velocities, i.e. the slip is also well controlled.

Here from Eqs. (1) and (3), the driving force, i.e. the friction force between the tire and the road surface, can be calculated as

$$F_d = \frac{T}{r} - \frac{J_w \dot{V}_w}{r^2} \tag{5}$$

In normal road conditions, F_d is less than the maximum friction force from the road and increases as T goes up. However, when slip occurs, F_d cannot increase by T. Thus when slip is occurring, the difference between the velocities of the wheel and the chassis become larger and larger, i.e. the acceleration of the wheel is larger than that of the chassis. Moreover, considering the μ – λ relation described in the Magic Formula, an appropriate difference between chassis velocity and wheel velocity is necessary to support the desired friction force. In this paper, α is defined as

$$\alpha = \frac{\dot{V}}{\dot{V}_w}, \text{ i.e. } \alpha = \frac{(F_d - F_{dr})/M}{(T_{\max} - rF_d)r/J_w} \tag{6}$$

It serves as a relaxation factor for smoothing the control system. In order to satisfy the condition that slip does not occur or become larger, α should be close to 1. With a designated α, when the vehicle encounters a slippery road, $T_{\max}$ must be reduced adaptively according to the decrease of F_d. If the friction force F_d is estimable, the maximum transmissible torque, $T_{\max}$ can be formulated as

$$T_{\max} = \left(\frac{J_w}{\alpha M r^2} + 1 \right) r \hat{F}_d \tag{7}$$

This formula indicates that a given estimated friction force $\hat{F}_d$ allows a certain maximum torque output from the wheel so as not to increase the slip. Hence, the MTTE scheme utilizes T_{max} to construct and constrain the driving torque T as

$$\begin{aligned} &-|T_{\max}| < T^* < |T_{\max}|, \; T = T^*; \\ &T^* \geq |T_{\max}|, \; T = |T_{\max}|; \\ &T^* \leq -|T_{\max}|, \; T = -|T_{\max}|. \end{aligned} \tag{8}$$

Note that from Eq. (2), it is clear that the driving resistance F_{dr} can be regarded as one of the perturbation sources of the dynamic vehicle mass M. Although the vehicle mass M can also be estimated online (Ikeda et al., 1992; Vahidi et al., 2005; Winstead & Kolmanovsky, 2005), in this paper, it is assumed to be a nominal value.

Figure 3 shows the main control scheme of the MTTE. As shown in Fig. 3, a limiter with a variable saturation value is expected to realize the control of driving torque according to the dynamic situation. The estimated disturbance force $\hat{F}_d$ is driven from the model inversion of the controlled plant and driving torque T. Consequently, a differentiator is needed. Under normal conditions, the torque reference is expected to pass through the controller without any effect. Conversely, when on a slippery road, the controller can constrain the torque output to be close to $T_{\max}$. Based on Eq. (7), an open-loop friction force estimator is employed based on the linear nominal model of the wheeled motor to produce the maximum transmissible torque. For practical convenience, two low pass filters (LPF) with the time constants of τ_1 and τ_2 respectively, are employed to smoothen the noises of digital signals and the differentiator which follows.

3. Disturbance estimation

The disturbance estimation is often employed in motion control to improve the disturbance rejection ability. Figure 4 shows the structure of open-loop disturbance estimation. As can be seen in this figure, we can obtain

$$\hat{T}_d = \left[\left(T^* + T_d \right) \left(G(s) + \Delta(s) \right) \right] G(s)^{-1} - T^* \tag{9}$$

If $\Delta(s) \neq 0$, then $\hat{T}_d \neq T_d$. Without the adjustment mechanism, the estimation accuracy decreases based on the deterioration of modeling error. Figure 5 shows the structure of closed-loop disturbance estimation. As seen in this figure, we can obtain

$$\hat{T}_d = C(s)\left[\left(G(s)+\Delta(s)\right)\left(T^* + T_d\right) - G(s)\left(T^* + \hat{T}_d\right)\right] \tag{10}$$

If $\Delta(s)=0$, Eq. (10) becomes a low pass dynamics as $\hat{T}_d = \dfrac{C(s)G(s)}{1+C(s)G(s)}T_d$. Moreover, from Eq. (10), without considering the feed-forward term of T^*, the closed-loop observer system of Eq. (10) can be reconstructed into a compensation problem as illustrated in Fig. 6. It is obvious that, the compensator $C(s)$ in the closed-loop structure offers a mechanism to minimize the modeling error caused by $\Delta(s)$ in a short time. Consequently, the compensator enhances the robust estimation performance against modeling error. Since the modeling error is unpredictable, the disturbance estimation based on closed-loop observer is preferred.

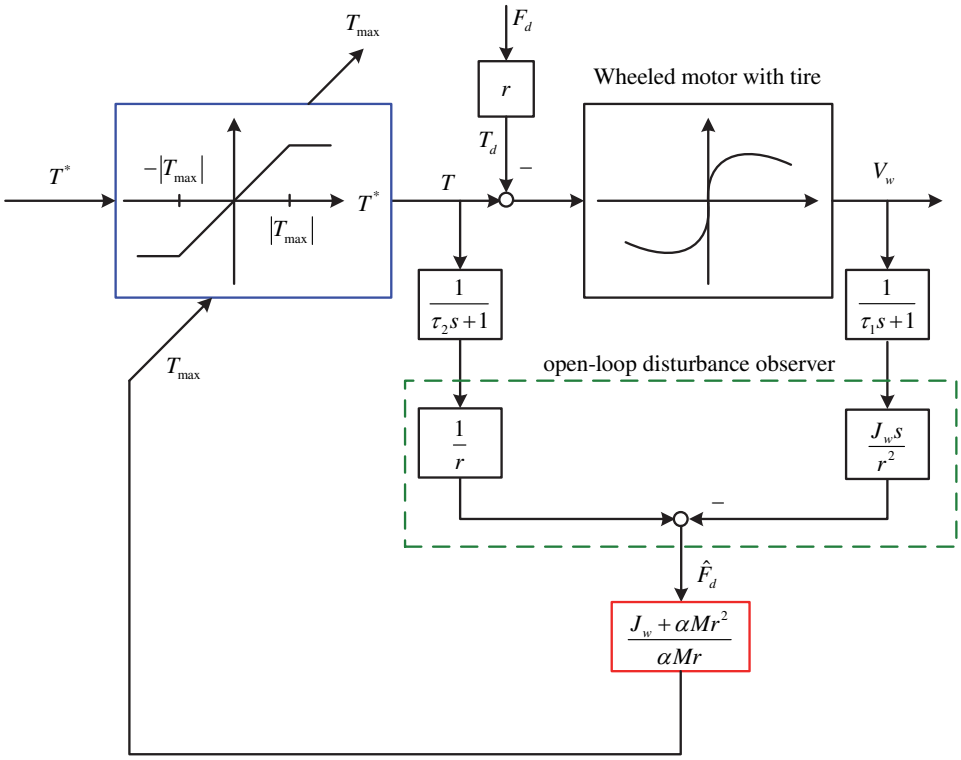

Fig. 3. Conventional MTTE system.

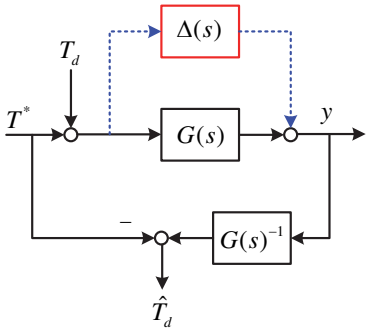

Fig. 4. Disturbance estimation based on open-loop observer.

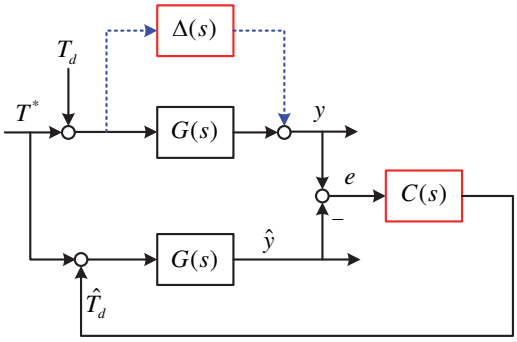

Fig. 5. Disturbance estimation based on closed-loop observer.

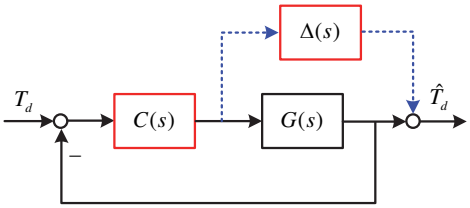

Fig. 6. Equivalent control block diagram of disturbance estimation.

4. Robustness analysis

Firstly, consider the conventional scheme of MTTE. The follow will show that the MTTE scheme is robust to the varying of vehicle mass. Note that the bandwidth of LPF is often designed to be double or higher than the system's bandwidth. Hence in motion control analysis, the LPFs can be ignored. Figure 7 shows a simplified linear model of MTTE scheme where M_n denotes the nominal value of vehicle mass M and $\Delta_d(s)$ stands for the perturbation caused by passenger and driving resistance F_{dr}. Here from Fig. 7, we have

$$\frac{T_{\max}}{F_d} = \frac{J_w}{\alpha M_n r} + r \tag{11}$$

Note that, if

$$\alpha M_n r \gg J_w \tag{12}$$

It is convinced that the condition of Eq. (12) is satisfied in most of the commercial vehicles. Then

$$\frac{T_{\max}}{F_d} \approx r \tag{13}$$

Now consider the mass perturbation of ΔM . From Eq. (11), it yields

$$\frac{T_{\max}}{F_d} = \frac{J_w}{\alpha\left(M_n + \Delta M\right) r} + r \tag{14}$$

Obviously, from Eq. (11), the anti-slip performance of MTTE will be enhanced when ΔM is a positive value and reduced when ΔM is a negative value. Additionally, in common vehicles, the MTTE approach is insensitive to the varying of M_n. Since passenger and driving resistance are the primary perturbations of M_n, the MTTE approach reveals its merits for general driving environments. The fact shows that the MTTE control scheme is robust to the varying of the vehicle mass M.

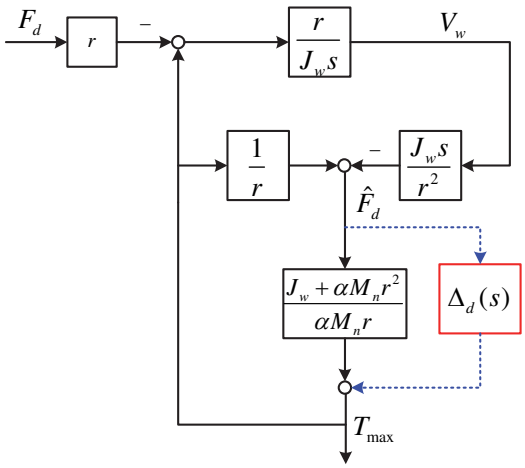

Fig. 7. Simplified MTTE control scheme.

Model uncertainty and sensor fault are the main faults concerned in this study. Since the conventional MTTE approach is based on the open-loop disturbance estimation, the system is hence sensitive to the varying of wheel inertia. If the tires are getting flat, the anti-slip performance of MTTE will deteriorate gradually. Figure 8 illustrates the advanced MTTE scheme which endows the MTTE with fault-tolerant performance. The disturbance torque

T_d comes from the operation friction. When the vehicle is operated on a slippery road, it causes the T_d to become very small, and due to that the tires cannot provide sufficient friction. Skidding often happens in braking and racing of an operated vehicle when the tire's adhesion cannot firmly grip the surface of the road. This phenomenon is often referred as the magic formula (i.e., the $\mu - \lambda$ relation). However, the $\mu - \lambda$ relation is immeasurable in real time. Therefore, in the advanced MTTE, the nonlinear behavior between the tire and road (i.e., the magic formula) is regarded as an uncertain source which deteriorates the steering stability and causes some abnormal malfunction in deriving.

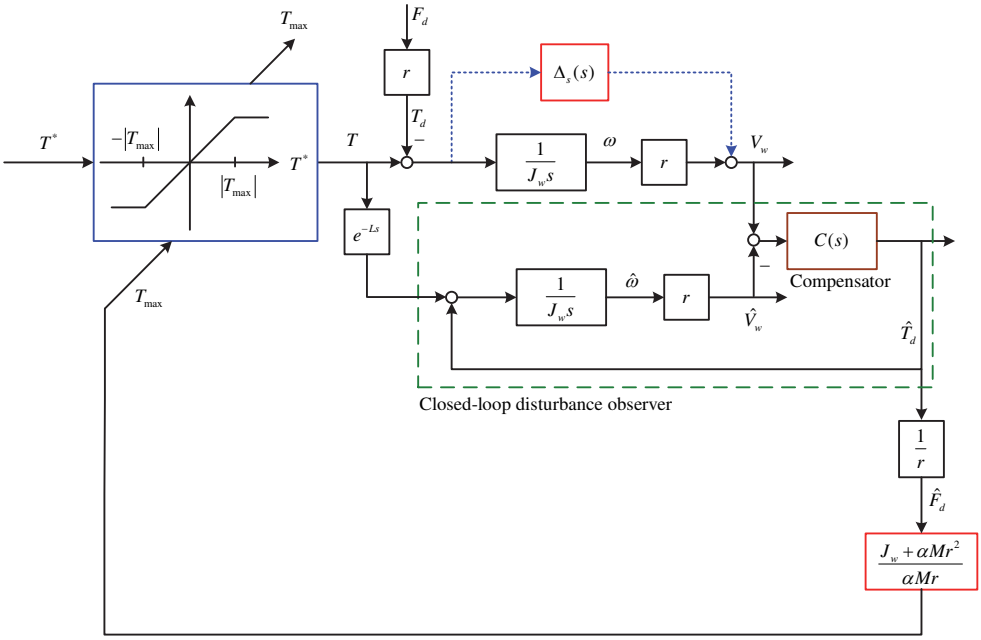

Fig. 8. Advanced MTTE control system.

Faults such as noise will always exist in a regular process; however not all faults will cause the system to fail. To design a robust strategy against different faults, the model uncertainties and system faults have to be integrated (Campos-Delgado et al., 2005). In addition, the sensor fault can be modeled as output model uncertainty (Hu & Tsai, 2008). Hence in this study, the model uncertainty and sensor fault are integrated as $\Delta_s(s)$ in the proposed system, which has significant affects to the vehicle skidding. Here, let $\Delta_s(s)$ denote the slip perturbation caused by model uncertainty and sensor fault on the wheeled motor. The uncertain dynamics of $\Delta_s(s)$ represent different slippery driving situations. When $\Delta_s(s) \approx 0$, it means the driving condition is normal. For a slippery road surface, the $\Delta_s(s) \neq 0$. It is commonly known that an open-loop disturbance observer has the following drawbacks.

1. An open-loop disturbance observer does not have a feedback mechanism to compensate for the modeling errors. Therefore its robustness is often not sufficient.

2. An open-loop disturbance observer utilizes the inversion of a controlled plant to acquire the disturbance estimation information. However, sometimes the inversion is not easy to carry out.

Due to the compensation of the closed-loop feedback, the closed-loop disturbance observer enhances the performance of advanced MTTE against skidding. It also offers better robustness against the parameter varying. Unlike the conventional MTTE approach, the advanced MTTE does not need to utilize the differentiator. Note that the advanced MTTE employs a closed-loop observer to counteract the effects of disturbance. Hence it is sensitive to the phase of the estimated disturbance. Consequently, the preview delay element e^{-Ls} is setup for compensating the digital delay of fully digital power electronics driver. This preview strategy coordinates the phase of the estimated disturbance torque.

The advanced MTTE is fault-tolerant against the model uncertainties and slightly sensor faults. Its verification is discussed in the following. Figure 9 shows a simplified linear model of the advanced MTTE scheme where J_{wn} denotes the nominal value of wheel inertia J_w and $\Delta_s(s)$ stands for the slippery perturbation caused by model uncertainties and sensor faults.

Formulate the proposed system into the standard control configuration as Fig. 10, the system's robustness reveals by determining $\|T_{zw}(s)\|_\infty \le \gamma$ such that $\|\Delta_s(s)\|_\infty < \frac{1}{\gamma}$. For convenience, the compensator employed in the closed-loop observer stage is set as

$$C(s) = K_p + K_i \frac{1}{s} \tag{15}$$

Note that the dynamics of delay element can be approximated as

$$e^{-Ls} \approx \frac{1}{1+Ls} \tag{16}$$

The delay time in practical system is less than 30ms. Hence it has higher bandwidth of dynamics than the vehicle system. Consequently, it can be omitted in the formulation. Then from Fig. 9, we have

$$T_{zw}(s) = \frac{T_{\max}}{F_d} = -\frac{K_p(J_{wn}+\alpha Mr^2)s + K_i(J_{wn}+\alpha Mr^2)}{J_{wn}\alpha Ms^2 + K_p\alpha Mrs + K_i\alpha Mr} \tag{17}$$

As stated in Section 2, α should be close to 1. Therefore, if

$$\alpha Mr^2 \gg J_{wn} \tag{18}$$

then Eq. (17) can be simplified as

$$\frac{T_{\max}}{F_d} = -\frac{K_p r^2 s + K_i r^2}{J_{wn}s^2 + K_p rs + K_i r} \tag{19}$$

It is convinced that the condition of Eq. (18) is satisfied in most commercial vehicles. Accordingly, when the anti-slip system confronts the Type I (Step type) or Type II (Ramp type) disturbances (Franklin et al., 1995), equation Eq. (19) can be further simplified as

$$\frac{T_{\max}}{F_d} \approx -r \tag{20}$$

This means the system of $\|T_{zw}\|_\infty \approx r$ is stable if and only if $\|\Delta_s(s)\|_\infty < \frac{1}{r}$.

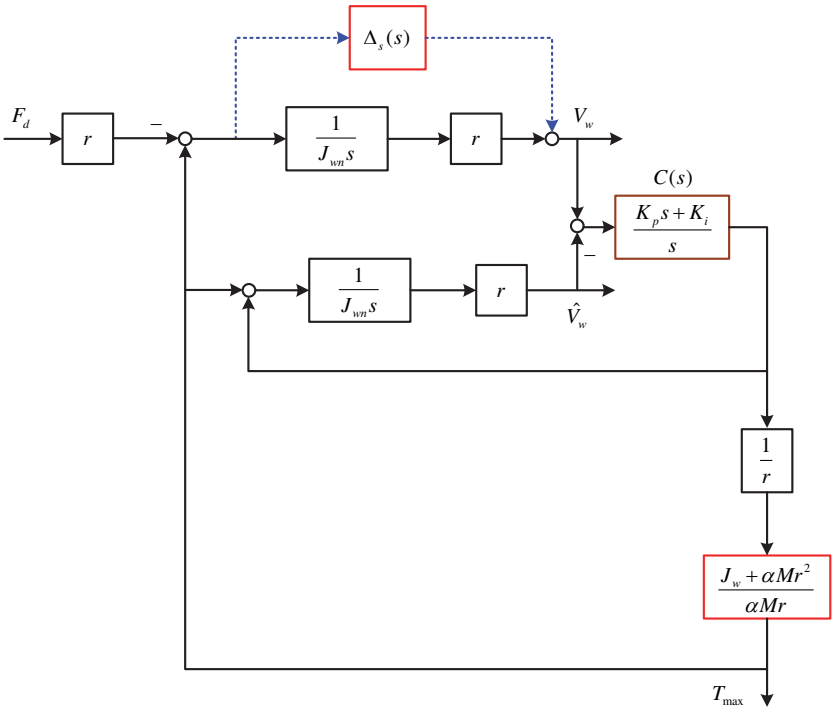

Fig. 9. A simplified scheme of proposed control.

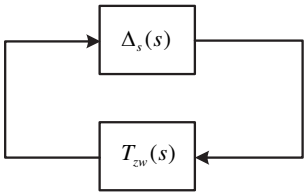

Fig. 10. Standard control configuration.

Now consider the affection of model uncertainty ΔJ_w to wheel inertia J_w. It yields $J_w = \Delta J_w + J_{wn}$. Since the mass of vehicle is larger than the wheels, in most of the commercial vehicle, $\alpha Mr^2 \gg \Delta J_w + J_{wn}$ is always held. Especially, the mass of passengers can also increase M to convince the condition of Eq. (18). Since the varying of J_w caused by ΔJ_w cannot affect the anti-slip control system so much. This means that the proposed control

approach for vehicle traction control is insensitive to the varying of J_w. Recall that the advanced MTTE scheme is MTTE-based. Consequently, by the discussions above, the proposed traction control approach reveals its fault-tolerant merits for dealing with certain dynamic modeling inaccuracies.

5. Examples and discussions

In order to implement and evaluate the proposed control system, a commercial electric vehicle, COMS3, which is assembled by TOYOTA Auto Body Co. Ltd., shown in Fig. 11 was modified to carry out the experiments' requirements. As illustrated in Fig. 12, a control computer is embedded to take the place of the previous Electronic Control Unit (ECU) to operate the motion control. The corresponding calculated torque reference of the left and the right rear wheel are independently sent to the inverter by two analog signal lines. Table 1 lists the main specifications.

Total Weight	360kg
Maximum Power/per wheel	2000W
Maximum Torque/per wheel	100Nm
Wheel Inertia/per wheel	0.5kgm^2
Wheel Radius	0.22m
Sampling Time	0.01s
Controller	Pentium M1.8G, 1GB RAM using Linux
A/D and D/A	12 bits
Shaft Encoder	36 pulses/round

Table 1. Specification of COMS3.

Fig. 11. Experimental electric vehicle and setting of slippery road for experiment.

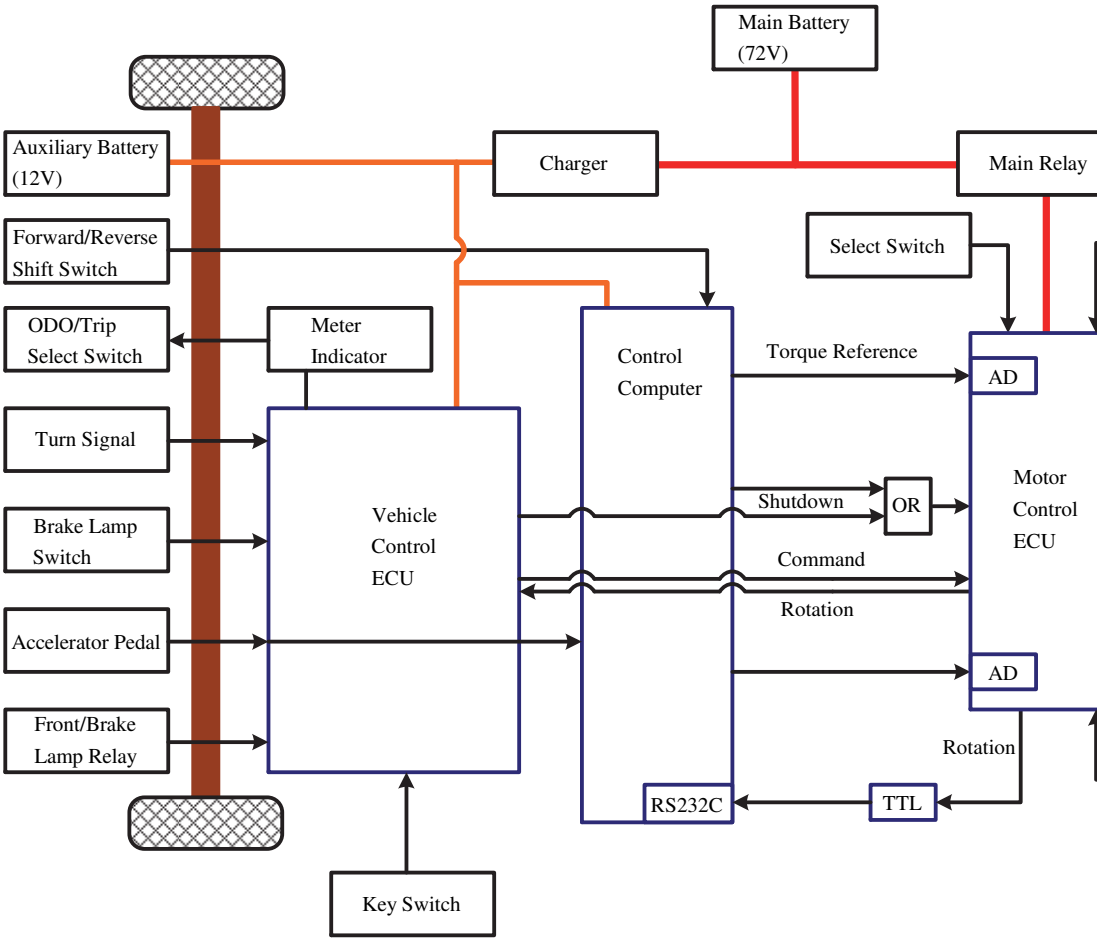
Main Battery
(72V)
Auxiliary Battery
(12V)
Charger
Main Relay
Forward/Reverse
Shift Switch
Select Switch
ODO/Trip
Select Switch
Meter
Indicator
Control
Computer
Torque Reference
AD
Turn Signal
Vehicle
Control
ECU
Shutdown
OR
Motor
Control
ECU
Brake Lamp
Switch
Command
Rotation
Accelerator Pedal
AD
Front/Brake
Lamp Relay
Rotation
RS232C
TTL
Key Switch

In the experiments, the relation factor of MTTE scheme is set as $\alpha = 0.9$. The time constants of LPFs in the comparison experiment are set as $\tau_1 = \tau_2 = 0.05$. It is known that the passenger's weight varies. Hence, this paper adopts the PI compensator as the kernel of disturbance estimation. The PI gains are set as $K_p = 70$, and $K_i = 60$. As shown in Fig. 11, the slippery road was set by an acrylic sheet with a length of 1.2m and lubricated with water. The initial velocity of the vehicle was set higher than 1m/s to avoid the immeasurable zone of the shaft sensors installed in the wheels. The driving torque delay in the advanced MTTE approach is exploited to adjust the phase of the estimated disturbance. Under a proper anti-slip control, the wheel velocity should be as closed to the chassis velocity as possible. As can be seen in Fig. 13, the advanced MTTE cannot achieve any anti-slip performance (i.e. the vehicle is skidded) if the reference signal is no delayed. Figure 13 also shows the measured results, and obviously, the digital delay of motor driver has significant affections to the advanced MTTE. According to the practical tests of Fig. 13, with proper command delay of 20ms, the advanced MTTE can achieve a feasible performance. Hence, in the following, all experiments to the advanced MTTE utilize this delay parameter.

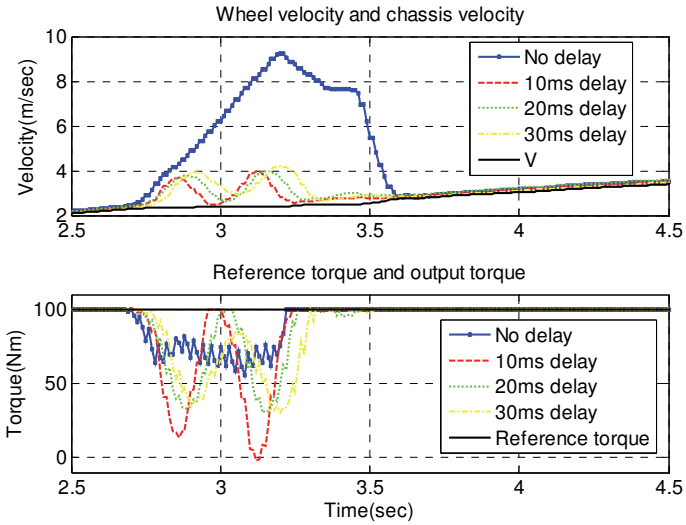

Fig. 13. Experimental results to different delay time L to advanced MTTE.

The MTTE-based schemes can prevent vehicle skid. These approaches compensate the reference torque into a limited value when encountering a slippery road. Based on the experimental result of Fig. 14, the reference torque of MTTE-based approaches is constrained without divergence. Figure 14 is evaluated under the nominal wheel inertia. As can be seen in this figure, both the conventional MTTE and advanced MTTE are with good anti-slip performance. Nevertheless, as indicated in the practical results in Fig. 15, the anti-slip performance of MTTE impairs with the varying of wheel inertia. In addition, Fig. 16 shows the same testing on the advanced MTTE. Apparently, the advanced MTTE overcomes this problem. The advanced MTTE has fault-tolerant anti-slip performance against the

wheel inertia varying in real time. Figures 17 and 18 show the performance tests of MTTE and advanced MTTE against different vehicle mass. It is no doubt that the MTTE-based control schemes are robust in spite of different passengers setting in the vehicle. From experimental evidences, it is evident that the advanced MTTE traction control approach has consistent performance to the varying of wheel inertia J_w and vehicle mass M. As shown in these figures, the proposed anti-slip system offers an effective performance in maintaining the driving stability under more common situations, and therefore the steering safety of the electric vehicles can be further enhanced.

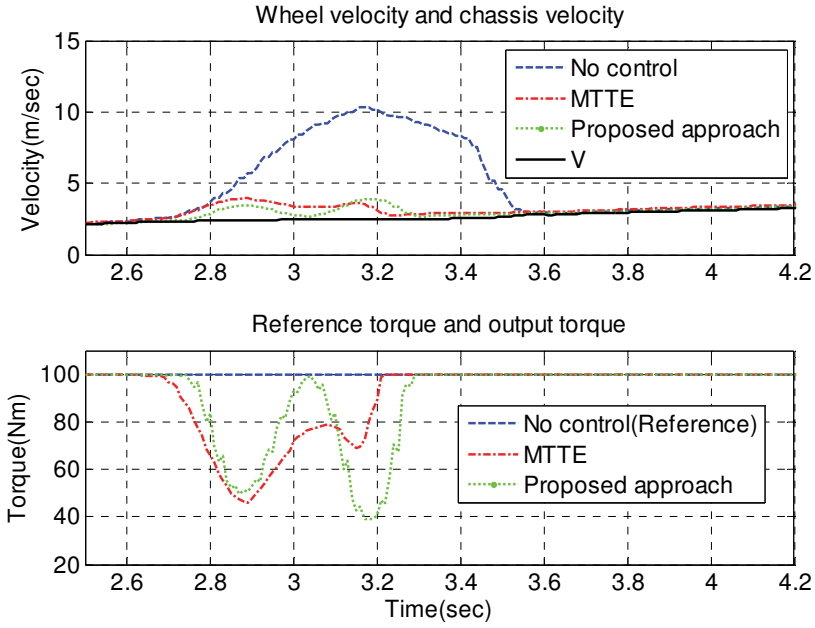

Fig. 14. Practical comparisons between MTTE and advanced MTTE to nominal J_w.

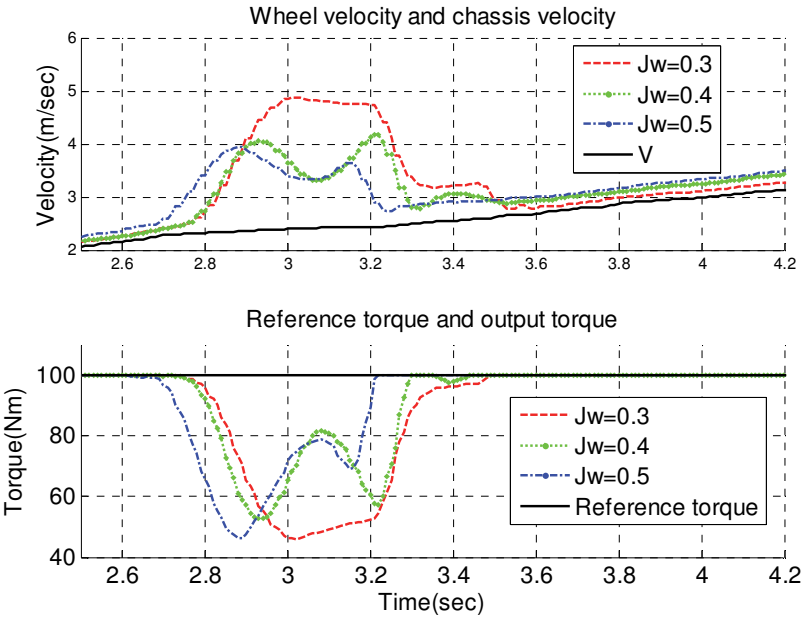

Fig. 15. Experimental results of MTTE to different J_w.

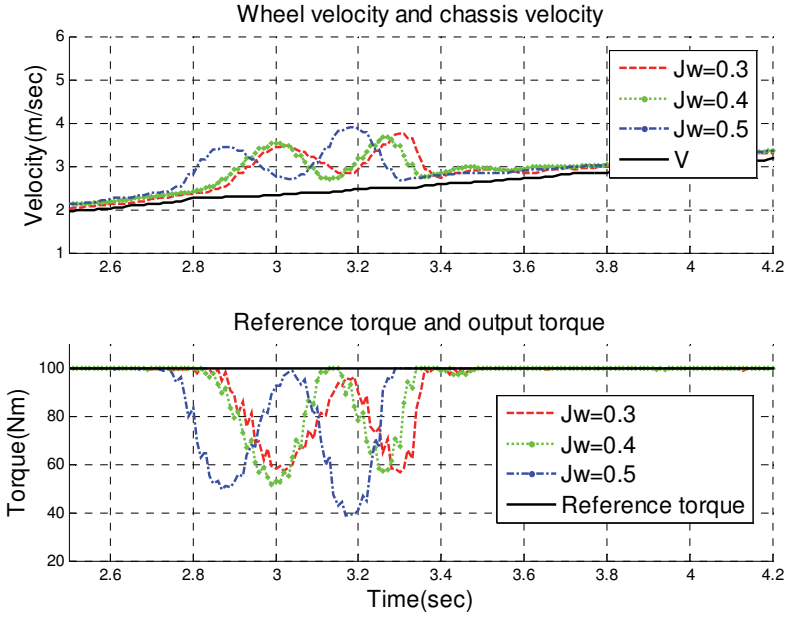

Fig. 16. Experimental results of advanced MTTE to different J_w.

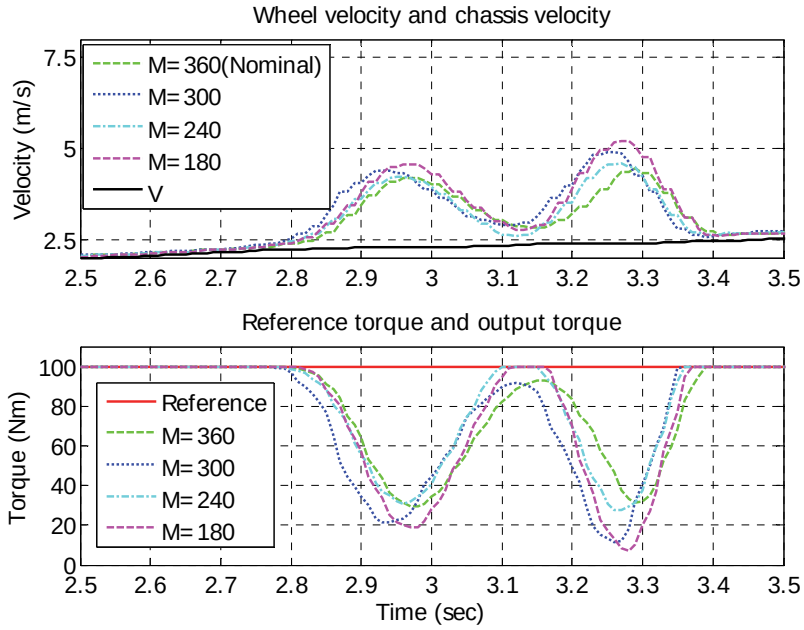

Fig. 17. Experimental results of MTTE to different M

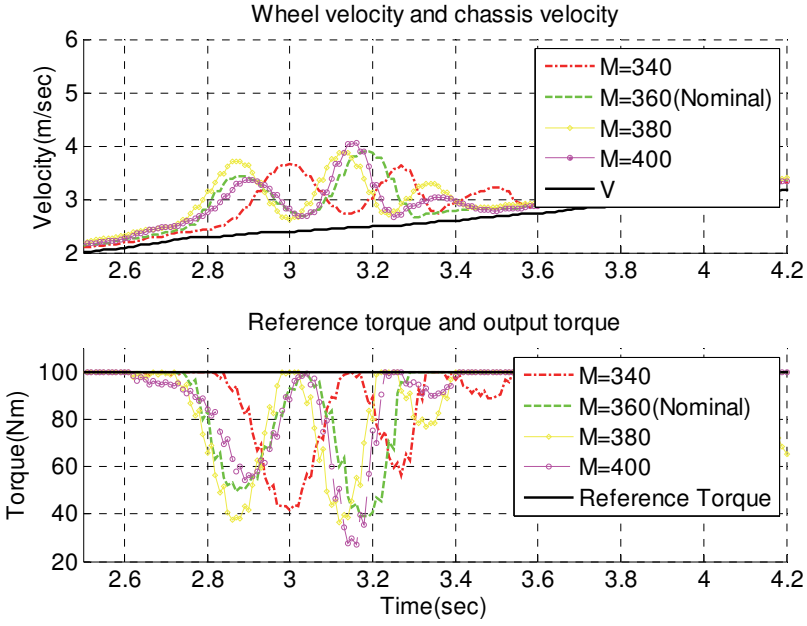

Fig. 18. Experimental results of advanced MTTE to different M

6. Conclusions

This paper has presented a robustness analysis to the traction control of MTTE based approach in electric vehicles. The schemes of conventional MTTE and advanced MTTE were introduced. The conventional MTTE was confirmed by analysis and experiment of its robustness to the perturbation of vehicle mass. This advanced MTTE endowed the conventional MTTE approach with a fault-tolerant ability for preventing driving skid of electric vehicles in many common steering situations. It provided a good basis for anti-slip control as well as other more advanced motion control systems in vehicles. The phase lag problem of disturbance estimation to closed-loop observer and digital implementation has been overcome by the driving torque delay in the advanced MTTE. The experimental results have substantiated that the advanced MTTE has benefits such as preventing potential failures in a slippery driving situation. In addition, the MTTE approaches have made cost effective traction control for electric vehicles possible.

7. Nomenclature

F_d	Friction Force (Driving Force)
F_{dr}	Driving Resistance
J_w	Wheel Inertia
M	Vehicle Mass
N	Vehicle Weight
r	Wheel Radius
T	Driving Torque
V	Chassis Velocity (Vehicle Velocity)
V_w	Wheel Velocity (Circumferential Velocity)
λ	Slip Ratio
μ	Friction Coefficient
ω	Wheel Rotation

8. References

Hori, Y. (2001). Future Vehicle Driven by Electricity and Control-research on four-wheel-motored "UOT electric march II. *IEEE Transactions on Industrial Electronics*, Vol.51, pp. 954-962.

He, P & Hori, Y. (2006). Optimum Traction Force Distribution for Stability Improvement of 4WD EV in Critical Driving Condition. *Proceedings of IEEE International Workshop on Advanced Motion Control*, pp. 596-601, Istanbul, Turkey.

Yang, Y.-P. & Lo, C.-P. (2008). Current Distribution Control of Dual Directly Driven Wheel Motors for Electric Vehicles. *Control Engineering Practice*, Vol.16, pp. 1285-1292.

Schinkel, M. & Hunt, K. (2002). Anti-lock Braking Control Using a Sliding Mode Like Approach, *Proceedings of the American Control Conference*, pp. 2386-2391, Anchorage, USA.

Patil, C. B.; Longoria, R. G. & Limroth, J. (2003). Control Prototyping for an Anti-lock Braking Control System on a Scaled Vehicle, *Proceedings of the IEEE Conference on Decision and Control*, pp. 4962-4967, Hawaii, USA.

Urakubo, T.; Tsuchiya, K. & Tsujita, K. (2001). Motion Control of a Two-wheeled Mobile Robot. *Advanced Robotics*, Vol.15, pp. 711-728.

Tsai, M.-C. & Hu, J.-S. (2007). Pilot Control of an Auto-balancing Two-wheeled Cart. *Advanced Robotics*, Vol.21, pp. 817-827.

Tahami, F.; Farhangi, S. & Kazemi, R. (2004). A Fuzzy Logic Direct Yaw-moment Control System for All-wheel-drive Electric Vehicles. *Vehicle System Dynamics*, Vol.41, pp. 203-221.

Mizushima, T.; Raksincharoensak, P. & Nagai, M. (2006). Direct Yaw-moment Control Adapted to Driver Behavior Recognition, *Proceedings of SICE-ICASE International Joint Conference*, pp. 534-539, Busan, Korea.

Bennett, S. M.; Patton, R. J. & Daley, S. (1999). Sensor Fault-tolerant Control of a Rail Traction Drive. *Control Engineering Practice*, Vol.7, pp. 217-225.

Poursamad, A. & Montazeri, M. (2008). Design of Genetic-fuzzy Control Strategy for Parallel Hybrid Electric Vehicles. *Control Engineering Practice*, Vol.16, pp. 861-873.

Mutoh, N.; Hayano, Y.; Yahagi, H. & Takita, K. (2007). Electric Braking Control Methods for Electric Vehicles with Independently Driven Front and Rear Wheels. *IEEE Transactions on Industrial Electronics*, Vol.54, pp. 1168-1176.

Baffet, G.; Charara, A. & Lechner, D. (2009) Estimation of Vehicle Sideslip, Tire Force and Wheel Cornering Stiffness. *Control Engineering Practice*, Vol. 17, pp. 1255-1264.

Saito, T.; Fujimoto, H. & Noguchi, T. (2002). Yaw-moment stabilization control of small electric vehicle, *Proceedings of the IEEJ Technical Meeting on Industrial Instrumentation and Control*, IIC-02, Tokyo, Japan.

Fujimoto, H.; Saito, T. & Noguchi, T. (2004). Motion stabilization control of electric vehicle under snowy conditions based on yaw-moment observer, *Proceedings of IEEE International Workshop on Advanced Motion Control*, pp. 35-40, Kawasaki, Japan.

Fujii K. & Fujimoto, H. (2007). Traction Control Based on Slip Ratio Estimation without Detecting Vehicle Speed for Electric Vehicle, *Proceedings of 4th Power Conversion Conference*, pp. 688-693, Nagoya, Japan.

Pacejka, H. B. & Bakker, E. (1992). The Magic Formula Tyre Model. *Vehicle System Dynamics*, Vol.21, pp. 1-18.

Sakai, S. & Hori, Y. (2001). Advantage of Electric Motor for Anti Skid Control of Electric Vehicle. *European Power Electronics Journal*, Vol.11, pp. 26-32.

Yin, D.; Hu, J.-S. & Hori, Y. (2009). Robustness Analysis of Traction Control Based on Maximum Transmission Torque Estimation in Electric Vehicles. *Proceedings of the IEEJ Technical Meeting on Industrial Instrumentation and Control*, IIC-09-027, Tokyo, Japan.

Patton, R. J.; Frank, P. M. & Clark., R. N. (2000). *Issues of Fault Diagnosis for Dynamic Systems*, Springer, New York, USA.

Campos-Delgado, D. U.; Martinez-Martinez, S. & Zhou, K. (2005). Integrated Fault-tolerant Scheme for a DC Speed Drive. *IEEE Transactions on Mechatronics*, Vol.10, pp. 419-427.

Ikeda, M.; Ono, T. & Aoki, N. (1992). Dynamic mass measurement of moving vehicles. *Transactions of the Society of Instrument and Control Engineers*, Vol.28, pp. 50-58.

Vahidi, A.; Stefanopoulou, A. & Peng, H. (2005). Recursive Least Squares with Forgetting for Online Estimation of Vehicle Mass and Road Grade: Theory and Experiments. *Vehicle System Dynamics*, Vol.43, pp. 31-55.

Winstead, V. & Kolmanovsky, I. V. (2005). Estimation of Road Grade and Vehicle Mass via Model Predictive Control, *Proceedings of IEEE Conference on Control Applications*, pp. 1588-1593, Toronto, Canada.

Hu, J.-S. & Tsai, M.-C. (2008). *Control and Fault Diagnosis of an Auto-balancing Two-wheeled Cart: Remote Pilot and Sensor/actuator Fault Diagnosis for Coaxial Two-wheeled Electric Vehicle*, VDM Verlag, Saarbrücken, Germany.

Franklin, G. F.; Powell, J. D. & Emami-Naeini, A. (1995). *Feedback Control of Dynamic Systems*, Addison Wesley, New York, USA.

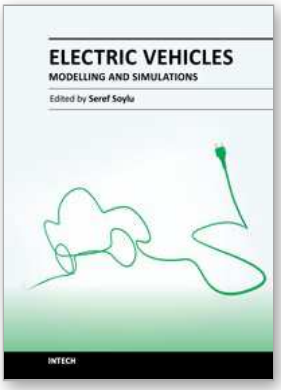

Electric Vehicles - Modelling and Simulations

Edited by Dr. Seref Soylu

ISBN 978-953-307-477-1
Hard cover, 466 pages
Publisher InTech
Published online 12, September, 2011
Published in print edition September, 2011

In this book, modeling and simulation of electric vehicles and their components have been emphasized chapter by chapter with valuable contribution of many researchers who work on both technical and regulatory sides of the field. Mathematical models for electrical vehicles and their components were introduced and merged together to make this book a guide for industry, academia and policy makers.

How to reference

In order to correctly reference this scholarly work, feel free to copy and paste the following:

Jia-Sheng Hu, Dejun Yin and Feng-Rung Hu (2011). A Robust Traction Control for Electric Vehicles Without Chassis Velocity, Electric Vehicles - Modelling and Simulations, Dr. Seref Soylu (Ed.), ISBN: 978-953-307-477-1, InTech, Available from: http://www.intechopen.com/books/electric-vehicles-modelling-and-simulations/a-robust-traction-control-for-electric-vehicles-without-chassis-velocity

INTECH
open science | open minds

InTech Europe
University Campus STeP Ri
Slavka Krautzeka 83/A
51000 Rijeka, Croatia
Phone: +385 (51) 770 447
Fax: +385 (51) 686 166
www.intechopen.com

InTech China
Unit 405, Office Block, Hotel Equatorial Shanghai
No.65, Yan An Road (West), Shanghai, 200040, China
中国上海市延安西路65号上海国际贵都大饭店办公楼405单元
Phone: +86-21-62489820
Fax: +86-21-62489821